

Variational Study of Asymmetric Nuclear Matter and a New Term in the Mass Formula

Masatoshi TAKANO and Masami YAMADA

*Advanced Research Institute for Science and Engineering, Waseda University,
Tokyo 169-8555, Japan*

(Received May 2, 2006)

Asymmetric nuclear matter at zero temperature is studied using a variational method which is an extension of the methods used by the present authors previously for simpler systems. An approximate expression for the energy per nucleon in asymmetric nuclear matter is derived through a combination of two procedures, one used for symmetric nuclear matter and the other for spin-polarized liquid ${}^3\text{He}$ with spin polarization replaced by isospin polarization. The approximate expression for the energy is obtained as a functional of various spin-isospin-dependent radial distribution functions, tensor distribution functions, and spin-orbit distribution functions. The Euler-Lagrange equations are derived to minimize this approximate expression for the energy; they consist of 16 coupled integrodifferential equations for various distribution functions. These equations were solved numerically for several values of the nucleon number density ρ and for many degrees of asymmetry ζ [$\zeta = (\rho_n - \rho_p)/\rho$, where ρ_n (ρ_p) is the neutron (proton) number density]. Unexpectedly, we find that the energies at a fixed density cannot be represented by a power series in ζ^2 . A new energy term, $\varepsilon_1(\zeta^2 + \zeta_0^2)^{1/2}$, where ζ_0 is a small number and ε_1 is a positive coefficient, is proposed. It is shown that if the power series is supplemented with this new term, it reproduces the energies obtained by variational calculations very accurately. This new term is studied in relation to cluster formation in nuclear matter, and some mention is made of a possible similar term in the mass formula for finite nuclei.

§1. Introduction

The variational study¹⁾ of infinite nuclear matter has a long history, and the results have been compared with other many-body calculations, such as the Brueckner-Hartree-Fock calculations. For asymmetric nuclear matter, which is the main object of our present study, there are fairly many studies employing nonrelativistic and relativistic Brueckner theories.²⁾ However, most variational calculations are for symmetric nuclear matter and neutron matter.³⁾ The variational calculations for asymmetric nuclear matter of which the author is aware are very few: the Fermi hypernetted chain (FHNC) calculations carried out in 1981,⁴⁾ and the lowest-order constrained variational (LOCV) calculations.⁵⁾

Since 1994, the present authors have been developing a different type of variational theory, in which approximate expressions for the energies per nucleon are constructed as functionals of various two-body distribution functions and structure functions. We now have approximate energy expressions for liquid ${}^3\text{He}$,⁶⁾ neutron matter, and symmetric nuclear matter.⁷⁾ For liquid ${}^3\text{He}$, we have an expression valid for arbitrary spin-polarized states.⁸⁾ In this paper, we extend the theory to treat asymmetric nuclear matter, utilizing the analogy between spin polarization and isospin polarization. Here, we should mention the guiding principle of these varia-

tional studies. We allow the variational functions to vary fully, without imposing any artificial constraint. Thus in order for our method to be successful, the approximate energy expression must have the property that its value remains in a reasonable range over the full variation of the variational functions.

In §2, we make a modification of the previously derived energy expression for the spin-polarized fermion system,⁸⁾ because we encountered a difficulty in treating spin-polarized neutron matter, and because we use the analogy between isospin polarization and spin polarization. In §3, we construct the approximate energy expression to be used for asymmetric nuclear matter, and the results of numerical calculations are presented. When we were analyzing the results, we found peculiar behavior of the energy per nucleon as a function of the degree of asymmetry ζ [$\zeta = (\rho_n - \rho_p)/\rho$, where ρ_n (ρ_p) is the neutron (proton) number density, and $\rho = \rho_n + \rho_p$]. We (and probably most researchers) had believed that the energy per nucleon at a fixed density ρ can be represented by a power series in ζ^2 . However, the results of our numerical calculations are contrary to this belief. In §4, a detailed analysis is presented to confirm the impossibility of a power series expansion. Furthermore, a new term, including a factor of $(\zeta^2 + \zeta_0^2)^{1/2}$, in which ζ_0 is a small number independent of ζ , is proposed. We find that if the power series is supplemented with this new term, it reproduces the results of the variational calculations very accurately. Since ζ_0 is very small, the range of ζ in which the power series in ζ^2 converges ($\zeta \leq \zeta_0$) is very narrow, indeed much narrower than the region of physical interest. The new term is discussed in relation to cluster formation in nuclear matter, and some mention is made of a possible similar term in the mass formula for finite nuclei. Brief concluding remarks are given in §5. In the appendix, results of the calculations for fictitious spin-polarized neutron matter that support the argument given in §4 are presented and discussed.

§2. Spin-polarized fermi liquid

2.1. Modification of the approximate energy expression

The main subject of this paper is asymmetric nuclear matter. In studying it, however, we have found that the formulas we proposed previously for polarized spin-1/2 fermion matter at zero temperature require some modification before treating asymmetric nuclear matter. The reason we need this modification beforehand is that the procedure for constructing the approximate energy expression for asymmetric nuclear matter is a generalization of the procedure for spin-polarized matter. We start from the Hamiltonian

$$H = - \sum_{i=1}^N \frac{\hbar^2}{2m} \nabla_i^2 + \sum_{i < j}^N \sum_{s=0}^1 V_s(r_{ij}) P_{sij}. \quad (2.1)$$

Here, N is the total number of particles, and m is the mass of a particle. The spin projection operator P_{sij} projects the (i, j) particle pair onto the spin-triplet state ($s = 1$) or the spin-singlet state ($s = 0$). The two-body central potential $V_s(r_{ij})$ with $\mathbf{r}_{ij} = \mathbf{r}_i - \mathbf{r}_j$ may depend on the spin state s . Because we consider infinite systems, both the particle number N and the volume Ω are taken to infinity, with the number

density $\rho = N/\Omega$ kept finite.

In the case of partially spin-polarized systems, the energy per particle, E/N , depends not only on ρ but also on $x = \rho_u/\rho$, with ρ_u being the number density of the spin-up particles. We also use $y = 1 - x$ in the following. In Ref. 8), we proposed an approximate energy expression for the energy per particle $E(\rho, x)/N$ as follows:

$$\begin{aligned} \frac{E}{N}(\rho, x) = & \frac{3}{5}(xE_{\text{Fu}} + yE_{\text{Fd}}) + 2\pi\rho \sum_{s=0}^1 \sum_{\mu} \int_0^{\infty} F_s^{\mu}(r)V_s(r)r^2 dr \\ & + \frac{\pi\hbar^2\rho}{2m} \sum_{s=0}^1 \sum_{\mu} \int_0^{\infty} \left[\frac{1}{F_s^{\mu}(r)} \frac{dF_s^{\mu}(r)}{dr} - \frac{1}{F_{\text{Fs}}^{\mu}(r)} \frac{dF_{\text{Fs}}^{\mu}(r)}{dr} \right]^2 F_s^{\mu}(r)r^2 dr \\ & - \frac{\hbar^2}{16\pi^2 m\rho} \sum_{n=1}^4 \int_0^{\infty} a_{cn} \frac{[S_{\text{cpn}}(k) - 1][S_{\text{cpn}}(k) - S_{\text{fn}}(k)]^2}{S_{\text{cpn}}(k)/S_{\text{fn}}(k)} k^4 dk + \frac{E_{3\text{corr}}}{N}. \end{aligned} \quad (2.2)$$

The first term on the right-hand side of Eq. (2.2) represents the one-body kinetic energy, where $E_{\text{Fu}} = \hbar^2 k_{\text{Fu}}^2/(2m)$ and $E_{\text{Fd}} = \hbar^2 k_{\text{Fd}}^2/(2m)$ are the Fermi energies for spin-up and spin-down Fermi spheres, respectively, with $k_{\text{Fu}} = (6\pi^2\rho x)^{1/3}$ and $k_{\text{Fd}} = (6\pi^2\rho y)^{1/3}$ being the corresponding Fermi wave numbers. The second term represents the potential energy, with the spin-dependent radial distribution functions $F_s^{\mu}(r)(s = 0, 1)$ defined by

$$F_s^{\mu}(r_{12}) = \Omega^2 \sum_{\text{spin}} \int \Psi^{\dagger}(x_1, \dots, x_N) P_{s_{12}}^{\mu} \Psi(x_1, \dots, x_N) dr_3 \cdots dr_N, \quad (2.3)$$

where $\Psi(x_1, \dots, x_N)$ is the wave function of the system, with x_i representing the space and spin coordinates of the i -th particle. The symbol \sum in Eq. (2.3) represents summation over the spin coordinates of all particles. The spin-projection operators $P_{s_{ij}}^{\mu}$ in Eq. (2.3) project the (i, j) particle pair onto the four spin states $(s, s_z) = (1, 1), (1, 0), (1, -1)$ or $(0, 0)$, where the superscript $\mu = (+, 0, -)$ indicates $s_z = (1, 0, -1)$, respectively. We should note that this second term is the exact expression for the expectation value of the potential energy per particle. The third and the fourth terms represent a part of the kinetic energy caused by correlations between particles. In the third term, $F_{\text{Fs}}^{\mu}(r)$ is the radial distribution function for the degenerate Fermi gas. In the fourth term, we have $(a_{c1}, a_{c2}, a_{c3}, a_{c4}) = (1, 1, x/y, y/x)$, and the various structure functions in this term are explained below.

The structure functions $S_{\text{cpn}}(k)(n = 1 - 4)$ are non-negative functions defined by

$$\begin{aligned} \left. \begin{aligned} S_{\text{cp1}}(k) \\ S_{\text{cp2}}(k) \end{aligned} \right\} &= 1 + \frac{S_1^+(k)}{2x} + \frac{S_1^-(k)}{2y} \\ &\mp \frac{1}{2} \sqrt{\left(\frac{S_1^+(k)}{x} - \frac{S_1^-(k)}{y} \right)^2 + \frac{(S_1^0(k) + S_0^0(k))^2}{xy}} \geq 0, \end{aligned} \quad (2.4a)$$

$$\left. \begin{array}{l} S_{\text{cp3}}(k) \\ S_{\text{cp4}}(k) \end{array} \right\} = 1 + \left(\begin{array}{c} 1 \\ \frac{2x}{1} \\ \frac{1}{2y} \end{array} \right) [S_1^0(k) - S_0^0(k)] \geq 0, \quad (2.4b)$$

where $S_s^\mu(k)$ are the Fourier transforms of $F_s^\mu(r)$:

$$S_s^\mu(k) = \rho \int [F_s^\mu(r) - F_s^\mu(\infty)] \exp(i\mathbf{k} \cdot \mathbf{r}) d\mathbf{r}, \quad (2.5)$$

for $(s, \mu) = (1, +), (1, 0), (1, -)$ and $(0, 0)$, respectively. The inequalities in (2.4) are necessary conditions on the structure functions, and, as discussed in Ref. 9), (2.4a) is equivalent to the following set of inequalities:

$$S_c^+(k) \equiv 1 + \frac{S_1^+(k)}{x} \geq 0, \quad (2.6a)$$

$$S_c^-(k) \equiv 1 + \frac{S_1^-(k)}{y} \geq 0, \quad (2.6b)$$

$$4xy S_c^+(k) S_c^-(k) - [S_1^0(k) + S_0^0(k)]^2 \geq 0. \quad (2.6c)$$

The functions $S_{fn}(k)$ in the fourth term on the right-hand side of Eq. (2.2) are defined by

$$S_{f1}(k) = S_{f2}(k) = x S_{\text{cF}}^+(k) + y S_{\text{cF}}^-(k) \equiv S_f(k), \quad (2.7a)$$

$$S_{fn}(k) \equiv S_{\text{cpFn}}(k), \quad (n = 3, 4) \quad (2.7b)$$

where $S_{\text{cF}}^\pm(k)$ and $S_{\text{cpFn}}(k)$ are, respectively, $S_c^\pm(k)$ and $S_{\text{cpn}}(k)$ for the degenerate Fermi gas. It should be noted that inequalities in (2.4) are automatically guaranteed in the variational calculations with the approximate energy expression Eq. (2.2).

The last term in Eq. (2.2) is a correction to the kinetic energy, and it is composed of two parts:

$$\frac{E_{3\text{corr}}}{N}(\rho, x) = \frac{E_{3\text{corr-01}}}{N}(\rho, x) + \frac{E_{3\text{corr-2}}}{N}(\rho, x). \quad (2.8)$$

The first part is

$$\begin{aligned} \frac{E_{3\text{corr-01}}}{N}(\rho, x) = \frac{\hbar^2}{16\pi^2 m \rho} \int_0^\infty \left\{ W_0(k) + \frac{W_1^+(k)}{x} [S_1^+(k) - S_{\text{F1}}^+(k)] \right. \\ \left. + \frac{W_1^-(k)}{y} [S_1^-(k) - S_{\text{F1}}^-(k)] \right\} k^4 dk, \end{aligned} \quad (2.9)$$

where

$$W_0(k) = \frac{[S_{\text{cF}}^+(k) - 1] [S_{\text{cF}}^+(k) - S_f(k)]^2}{S_{\text{cF}}^+(k) / S_f(k)}$$

$$+ \frac{[S_{\text{cF}}^-(k) - 1] [S_{\text{cF}}^-(k) - S_{\text{f}}(k)]^2}{S_{\text{cF}}^-(k)/S_{\text{f}}(k)}, \quad (2.10a)$$

$$W_1^\pm(k) = \frac{S_{\text{f}}(k) [S_{\text{cF}}^\pm(k) - S_{\text{f}}(k)]}{[S_{\text{cF}}^\pm(k)]^2} \left\{ 2 [S_{\text{cF}}^\pm(k)]^2 - S_{\text{cF}}^\pm(k) - S_{\text{f}}(k) \right\}, \quad (2.10b)$$

with $S_{\text{F}_s}^\mu(k)$ being $S_s^\mu(k)$ for the degenerate Fermi gas. The last term in Eq. (2.8) is expressed as

$$\begin{aligned} \frac{E_{3\text{corr-2}}}{N}(\rho, x) = & -\frac{\hbar^2}{16\pi^2 m \rho} \int_0^\infty \left\{ W_2^+(k) [S_{\text{c}}^+(k) - S_{\text{cF}}^+(k)]^2 \right. \\ & + W_2^-(k) [S_{\text{c}}^-(k) - S_{\text{cF}}^-(k)]^2 \\ & \left. + \frac{W_2^0(k)}{xy} [S_1^0(k) + S_0^0(k)]^2 \right\} k^4 dk, \end{aligned} \quad (2.11)$$

where

$$W_2^\pm(k) = S_{\text{cF}}^\pm(k) - 1 - S_{\text{f}}(k) + \left[\frac{S_{\text{f}}(k)}{S_{\text{cF}}^\pm(k)} \right]^3, \quad (2.12a)$$

$$\begin{aligned} W_2^0(k) = & \frac{1}{4} \left[S_{\text{cF}}^+(k) + S_{\text{cF}}^-(k) - 2 \right. \\ & \left. - S_{\text{f}}(k) \left\{ 2 - \left[\frac{S_{\text{f}}(k)}{S_{\text{cF}}^+(k)S_{\text{cF}}^-(k)} \right]^2 [S_{\text{cF}}^+(k) + S_{\text{cF}}^-(k)] \right\} \right]. \end{aligned} \quad (2.12b)$$

In Ref. 8), we carried out variational calculations using these expressions for liquid ^3He , and we obtained fairly reasonable results. However, we later encountered a case in which the numerically minimized energy obtained from the expression Eq. (2.2) is unreasonably low; specifically, $E_{3\text{corr-2}}(\rho, x)/N$ became a large negative value. Following the guiding principle mentioned in §1, we modify the approximate energy expression to avoid this unreasonable lowering of the kinetic energy.*) Specifically, we need to modify the expression for $E_{3\text{corr-2}}(\rho, x)/N$, which was found to be responsible for this energy lowering.

A convenient way to avoid the unreasonable lowering of the kinetic energy is to put a denominator in the dangerous term. The necessary conditions on such a denominator are that it be nonnegative, that it increase as the numerator increases, and that it tend to unity as the system tends to the degenerate Fermi gas, so that the correspondence between our formalism and the cluster expansion is unchanged up to the main part of the three-body clusters.

With the above considerations, the modified expression we propose for $E_{3\text{corr-2}}(\rho, x)/N$ is as follows:

$$\frac{E_{3\text{corr-2}}}{N}(\rho, x) = -\frac{\hbar^2}{16\pi^2 m \rho} \int_0^\infty \left\{ W_2^+(k) \frac{[S_{\text{c}}^+(k) - S_{\text{cF}}^+(k)]^2}{S_{\text{c}}^+(k)/S_{\text{cF}}^+(k)} \right.$$

*) The kinetic energy cannot be lower than the kinetic energy of the degenerate Fermi gas.

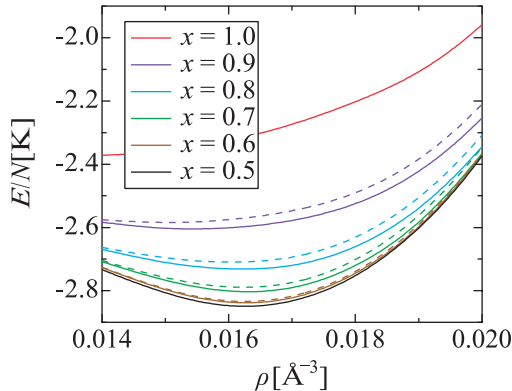


Fig. 1. Energies per particle, E/N , for liquid ${}^3\text{He}$ as functions of the number density ρ with the fraction of spin-up particles $x = 0.5, 0.6, 0.7, 0.8, 0.9$, and 1 . The solid curves represent the energies calculated with the modified energy expression, while the dotted curves are for the unmodified expression.

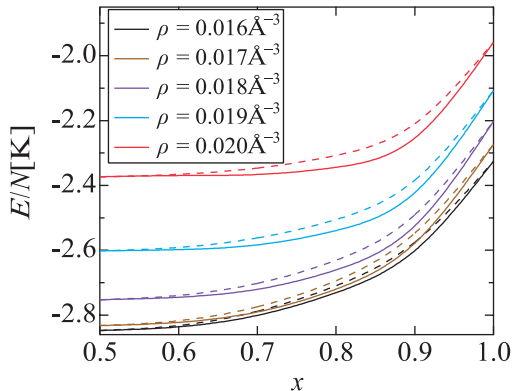


Fig. 2. Energies per particle, E/N , for liquid ${}^3\text{He}$ as functions of the fraction of spin-up particles x with $\rho = 0.016, 0.017, 0.018, 0.019$, and 0.020 \AA^{-3} . The solid curves and dotted curves represent the modified and unmodified expressions, respectively, as in Fig. 1.

$$+W_2^-(k) \left\{ \frac{[S_c^-(k) - S_{cF}^-(k)]^2}{S_c^-(k)/S_{cF}^-(k)} + \frac{W_2^0(k)}{xy} [S_1^0(k) + S_0^0(k)]^2 \right\} k^4 dk. \quad (2.13)$$

In the integrand of Eq. (2.13), the denominators in the first two terms satisfy the above-mentioned conditions, while no suitable denominator is found for the third term, which is not responsible for the unreasonable energy lowering.

2.2. Numerical calculations for spin-polarized liquid ${}^3\text{He}$

Once the approximate energy expression is constructed, we can derive the Euler-Lagrange (EL) equations through the variational procedure. In this case, the variational functions are spin-dependent radial distribution functions $F_s^\mu(r)$, and the EL equations are coupled integrodifferential equations for $F_s^\mu(r)$. We can solve them numerically with the iteration method explained in detail in Ref. 6).

In this subsection, we test the modified energy expression obtained in the last subsection with spin-polarized liquid ${}^3\text{He}$. We use Eq. (2.2) with the mass of a ${}^3\text{He}$ atom as m . The potential $V_s(r)$ corresponds to the intermolecular force between two ${}^3\text{He}$ atoms; in this paper, we use the HFDHE2 potential.¹⁰⁾

The energy per particle, E/N , is plotted in Figs. 1 and 2 with the old and modified expressions, Eqs. (2.11) and (2.13). It is seen that, in this case, the essential feature of E/N is not changed by the modification. A somewhat significant change is seen in the highly, but not completely, spin-polarized region ($x \approx 0.9$), where the modified E/N values are appreciably lower than the old ones. Figures 3 and 4 present some examples of the spin-dependent radial distribution functions $F_s^\mu(r)$ and the structure functions $S_{c\text{pn}}(k)$ for the modified energy expression. These functions are almost

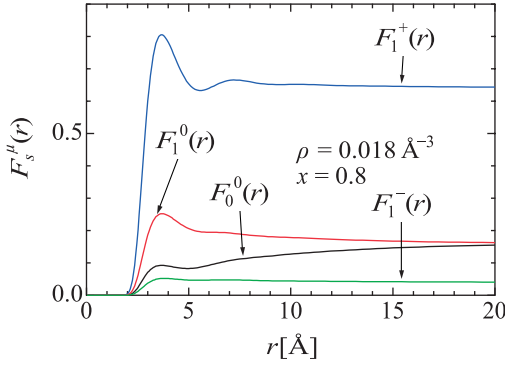


Fig. 3. Radial distribution functions $F_s^\mu(r)$ for liquid ${}^3\text{He}$ at $\rho = 0.018 \text{ \AA}^{-3}$, $x = 0.8$.

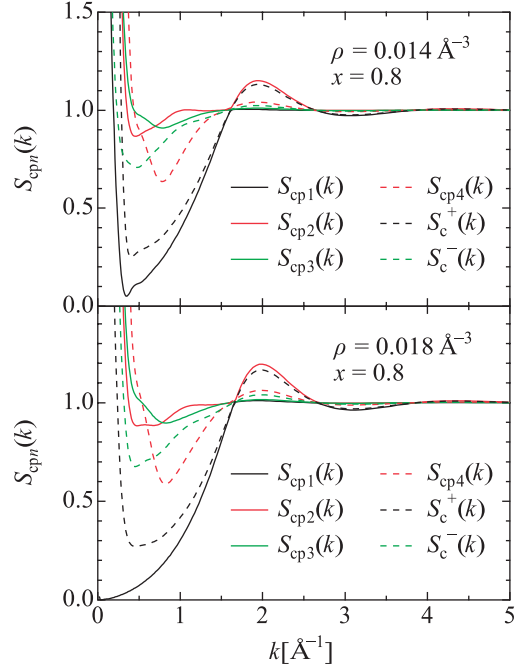


Fig. 4. Structure functions $S_{\text{cp}n}(k)$ for liquid ${}^3\text{He}$ at $\rho = 0.014 \text{ \AA}^{-3}$ and $\rho = 0.018 \text{ \AA}^{-3}$, with $x = 0.8$. The functions $S_c^\pm(k)$ defined in Eqs. (2-6) are also shown.

the same as those obtained with the old expression: The long tails of $F_s^\mu(r)$ and the increases of $S_{\text{cp}n}(k)$ near $k \approx 0$ are similar to those found without the modification.

§3. Approximate energy expression for asymmetric nuclear matter

3.1. Formulation for asymmetric nuclear matter

In this subsection, we construct an approximate energy expression for spin-unpolarized asymmetric nuclear matter at zero temperature. The procedure we employ here is a combination of two procedures, one for symmetric nuclear matter, which is explained in Ref. 7), and the other for spin-polarized liquid ${}^3\text{He}$, which is presented in Ref. 8) and modified in the last section. The ‘‘spin polarization’’ in the latter procedure is replaced here by ‘‘isospin polarization’’. Hereafter, we assign isospin-up to protons and isospin-down to neutrons.

We start from the Hamiltonian

$$H = - \sum_{i=1}^N \frac{\hbar^2}{2m} \nabla_i^2 + \sum_{i<j}^N V_{ij}, \quad (3.1)$$

where m is the nucleon mass, defined as the average of the proton mass and the

neutron mass. The two-body potential V_{ij} is assumed to be expressed as

$$V_{ij} = \sum_{t=0}^1 \sum_{s=0}^1 \{ [V_{Cts}(r_{ij}) + s [V_{Tt}(r_{ij})S_{Tij} + V_{SOt}(r_{ij}) (\mathbf{s} \cdot \mathbf{L}_{ij})]] P_{tsij} \} + V_{qij}. \quad (3.2)$$

Here, the operators P_{tsij} are the isospin-spin-projection operators, which project the (i, j) nucleon pair states onto the triplet-odd $[(t, s) = (1, 1)]$, singlet-even $[(t, s) = (1, 0)]$, triplet-even $[(t, s) = (0, 1)]$ or singlet-odd $[(t, s) = (0, 0)]$ state, S_{Tij} is the tensor operator,

$$S_{Tij} = \frac{3}{r_{ij}^2} (\boldsymbol{\sigma}_i \cdot \mathbf{r}_{ij})(\boldsymbol{\sigma}_j \cdot \mathbf{r}_{ij}) - \boldsymbol{\sigma}_i \cdot \boldsymbol{\sigma}_j, \quad (3.3)$$

\mathbf{L}_{ij} is the relative orbital angular momentum of the (i, j) nucleon pair, and V_{qij} is a quadratic angular momentum part. For the isoscalar part^{*)} of the AV18 potential,⁽¹¹⁾ we have

$$V_{qij} = \sum_{t=0}^1 \sum_{s=0}^1 \left[V_{qLts}(r_{ij}) |\mathbf{L}_{ij}|^2 + s V_{qSOt}(r_{ij}) (\mathbf{s} \cdot \mathbf{L}_{ij})^2 \right] P_{tsij}. \quad (3.4)$$

For simplicity, in this paper, we omit the remaining isovector and isotensor parts included in the AV18 potential, as in the case of the FHNC calculations of Akmal et al.,⁽³⁾ because their contribution to the total energy is expected to be negligibly small.

We construct the approximate energy expression for asymmetric nuclear matter as a functional of the spin-isospin-dependent radial distribution functions $F_{ts}^\nu(r)$, tensor distribution functions $F_{Tt}^\nu(r)$, and the spin-orbit distribution functions $F_{SOt}^\nu(r)$, which depend on the z -component, t_z , of the total isospin of the two participating nucleons:

$$F_{ts}^\nu(r_{12}) = \Omega^2 \sum_{\text{isospin}} \sum_{\text{spin}} \int \Psi^\dagger(x_1, \dots, x_N) P_{ts12}^\nu \Psi(x_1, \dots, x_N) d\mathbf{r}_3 \cdots d\mathbf{r}_N, \quad (3.5a)$$

$$F_{Tt}^\nu(r_{12}) = \Omega^2 \sum_{\text{isospin}} \sum_{\text{spin}} \int \Psi^\dagger(x_1, \dots, x_N) S_{T12} P_{t112}^\nu \Psi(x_1, \dots, x_N) d\mathbf{r}_3 \cdots d\mathbf{r}_N, \quad (3.5b)$$

$$F_{SOt}^\nu(r_{12}) = \Omega^2 \sum_{\text{isospin}} \sum_{\text{spin}} \int \Psi^\dagger(x_1, \dots, x_N) (\mathbf{s} \cdot \mathbf{L}_{12}) P_{t112}^\nu \Psi(x_1, \dots, x_N) d\mathbf{r}_3 \cdots d\mathbf{r}_N. \quad (3.5c)$$

Here, the summations are taken over the spin and isospin coordinates of all nucleons, and $\nu = (+, 0, -)$ represents the three isotriplet states, $t_z = (1, 0, -1)$, of the nucleon pair. In Eq. (3.5), P_{tsij}^ν is the corresponding projection operator.

The distribution functions in Eq. (3.5) implicitly depend on the proton fraction $\xi = \rho_p/\rho$ which is the ratio of the proton number density, ρ_p , to the total nucleon

^{*)} Here, the isoscalar part means the charge-independent part, which is by far the dominant part of the nuclear potential. Note that this is not the part pertinent to the isospin-singlet state.

number density, ρ . We also use the neutron fraction $\eta = \rho_n/\rho$, where ρ_n is the neutron number density. The asymmetry parameter ζ introduced in §1 is related to ξ and η as $\zeta = 1 - 2\xi = 2\eta - 1$. In this paper, we mainly treat the case $\xi \leq \eta$ in the range from $\xi = 1/2$ (symmetric nuclear matter, for which $\zeta = 0$) to $\xi = 0$ (neutron matter, for which $\zeta = 1$).

In order to construct the approximate energy expression, we temporarily assume a Jastrow-type wave function,

$$\Psi(x_1, \dots, x_N) = \text{Sym} \left[\prod_{i < j} f_{ij} \right] \Phi_F(x_1, \dots, x_N), \quad (3.6)$$

where $\text{Sym}[\]$ is the symmetrizer with respect to the order of the factors in the products, and $\Phi_F(x_1, \dots, x_N)$ is the wave function of the degenerate Fermi gas. The correlation function f_{ij} in Eq. (3.6) is taken as

$$f_{ij} = \sum_{t=0}^1 \sum_{s=0}^1 \sum_{\nu} [f_{Cts}^{\nu}(r_{ij}) + s f_{Tt}^{\nu}(r_{ij}) S_{Tij} + s f_{SOt}^{\nu}(r_{ij}) (\mathbf{s} \cdot \mathbf{L}_{ij})] P_{tsij}^{\nu}. \quad (3.7)$$

It should be noted that, after the approximate energy expression is constructed, this temporary assumption concerning the wave function is removed. Then, we cluster-expand both the expectation value of the Hamiltonian $\langle H \rangle / N$ ($\langle H \rangle \equiv \langle \Psi | H | \Psi \rangle / \langle \Psi | \Psi \rangle$) and the distribution functions appearing in Eq. (3.5). In the two-body cluster approximation, they are expressed as explicit functionals of the correlation functions $f_{Cts}^{\nu}(r)$, $f_{Tt}^{\nu}(r)$ and $f_{SOt}^{\nu}(r)$. By eliminating these correlation functions, in principle, the two-body cluster approximation of $\langle H \rangle / N$ can be expressed in terms of the distribution functions. In practice, however, we have to rely on auxiliary functions, i.e., “intrinsically-central distribution functions” $F_{Cts}^{\nu}(r)$, “dressed tensor correlation functions” $g_{Tt}^{\nu}(r)$, and “dressed spin-orbit correlation functions” $g_{SOt}^{\nu}(r)$, defined as the solutions of the following set of equations:

$$F_{ts}^{\nu}(r) = F_{Cts}^{\nu}(r) + 8s [g_{Tt}^{\nu}(r)]^2 F_{Fts}^{\nu}(r) + \frac{2}{3}s [g_{SOt}^{\nu}(r)]^2 F_{qFts}^{\nu}(r), \quad (3.8a)$$

$$F_{Tt}^{\nu}(r) = 16 \left\{ \sqrt{F_{Ct1}^{\nu}(r) F_{Ft1}^{\nu}(r)} g_{Tt}^{\nu}(r) - [g_{Tt}^{\nu}(r)]^2 F_{Ft1}^{\nu}(r) \right\} - \frac{2}{3} [g_{SOt}^{\nu}(r)]^2 F_{qFt1}^{\nu}(r), \quad (3.8b)$$

$$F_{SOt}^{\nu}(r) = -24 [g_{Tt}^{\nu}(r)]^2 F_{Ft1}^{\nu}(r) + \frac{4}{3} \left\{ \sqrt{\frac{F_{Ct1}^{\nu}(r)}{F_{Ft1}^{\nu}(r)}} g_{SOt}^{\nu}(r) - \frac{[g_{SOt}^{\nu}(r)]^2}{4} - g_{Tt}^{\nu}(r) g_{SOt}^{\nu}(r) \right\} F_{qFt1}^{\nu}(r). \quad (3.8c)$$

Here, $F_{Fts}^{\nu}(r)$ is the radial distribution function in the case of the degenerate Fermi gas, and explicitly, it is given by

$$F_{Fts}^{\nu}(r) = \frac{w_t^{\nu}(2s+1)}{4} \{ 1 - (-1)^{t+s} l(z_1) l(z_2) \}, \quad (3.9)$$

where $(w_1^+, w_1^0, w_1^-, w_0^0) = (\xi^2, \xi\eta, \eta^2, \xi\eta)$, $l(z) \equiv 3 j_1(z)/z$, and $z_1 = z_2 = k_{Fp}r$ for $(t, \nu) = (1, +)$, $z_1 = z_2 = k_{Fn}r$ for $(t, \nu) = (1, -)$, and $(z_1, z_2) = (k_{Fp}r, k_{Fn}r)$ for

$\nu = 0$, with $k_{Fp} = (3\pi^2\rho\xi)^{1/3}$ and $k_{Fn} = (3\pi^2\rho\eta)^{1/3}$ being the Fermi wave numbers for protons and neutrons. Furthermore, $F_{qFts}^\nu(r)$ is also a function pertinent to the degenerate Fermi gas:

$$\begin{aligned} F_{qFts}^\nu(r_{12}) &= \Omega^2 \sum_{\text{isospin}} \sum_{\text{spin}} \int \Phi_F^\dagger(x_1, \dots, x_N) |\mathbf{L}_{12}|^2 P_{ts12}^\nu \Phi_F(x_1, \dots, x_N) d\mathbf{r}_3 \cdots d\mathbf{r}_N \\ &= \frac{w_t^\nu(2s+1)}{4} \left\{ \frac{(z_1)^2 + (z_2)^2}{10} + (-1)^{t+s} \frac{3}{2} [j_2(z_1)l(z_2) + j_2(z_2)l(z_1)] \right\}, \end{aligned} \quad (3.10)$$

where the choice of z_1 and z_2 is the same as in the case of Eq. (3.9), except that r is replaced by r_{12} .

Using the auxiliary functions, the two-body cluster approximation of $\langle H \rangle / N$ can be expressed as follows:

$$\begin{aligned} \frac{\langle H \rangle_2}{N}(\rho, \zeta) &\approx \frac{E_2}{N}(\rho, \zeta) = \frac{3}{5} (\xi E_{Fp} + \eta E_{Fn}) \\ &+ 2\pi\rho \sum_{t=0}^1 \sum_{s=0}^1 \sum_{\nu} \int_0^\infty [F_{ts}^\nu(r) V_{Cts}(r) + s F_{Tt}^\nu(r) V_{Tt}(r) \\ &+ s F_{SOt}^\nu(r) V_{SOt}(r) + F_{qLts}^\nu(r) V_{qLts}(r) + s F_{qSOt}^\nu(r) V_{qSOt}(r)] r^2 dr \\ &+ \frac{2\pi\hbar^2\rho}{m} \sum_{t=0}^1 \sum_{s=0}^1 \sum_{\nu} \int_0^\infty \left\{ \left[\frac{1}{F_{Cts}^\nu(r)} \frac{dF_{Cts}^\nu(r)}{dr} - \frac{1}{F_{Fts}^\nu(r)} \frac{dF_{Fts}^\nu(r)}{dr} \right]^2 \right. \\ &\times \frac{F_{Cts}^\nu(r)}{4} + 8s \left\{ \left[\frac{dg_{Tt}^\nu(r)}{dr} \right]^2 + \frac{6}{r^2} [g_{Tt}^\nu(r)]^2 \right\} F_{Ft1}^\nu(r) \\ &\left. + \frac{2s}{3} \left[\frac{dg_{SOt}^\nu(r)}{dr} \right]^2 F_{qFt1}^\nu(r) \right\} r^2 dr. \end{aligned} \quad (3.11)$$

Here, $E_{Fp} = \hbar^2 k_{Fp}^2 / (2m)$ and $E_{Fn} = \hbar^2 k_{Fn}^2 / (2m)$ are the Fermi energies for the protons and neutrons, respectively. In addition, we have

$$\begin{aligned} F_{qLts}^\nu(r) &= F_{Cts}^\nu(r) \frac{F_{qFts}^\nu(r)}{F_{Fts}^\nu(r)} + 8s [g_{Tt}^\nu(r)]^2 [6F_{Fts}^\nu(r) + F_{qFts}^\nu(r)] \\ &+ \frac{2}{3} s [g_{SOt}^\nu(r)]^2 F_{bFts}^\nu(r), \end{aligned} \quad (3.12a)$$

$$\begin{aligned} F_{qSOt}^\nu(r) &= \frac{2}{3} F_{Ct1}^\nu(r) \frac{F_{qFt1}^\nu(r)}{F_{Ft1}^\nu(r)} - \frac{2}{3} \sqrt{\frac{F_{Ct1}^\nu(r)}{F_{Ft1}^\nu(r)}} [2g_{Tt}^\nu(r) + g_{SOt}^\nu(r)] F_{qFt1}^\nu(r) \\ &+ [g_{Tt}^\nu(r)]^2 \left[72F_{Ft1}^\nu(r) + \frac{20}{3} F_{qFt1}^\nu(r) \right] + \frac{8}{3} g_{Tt}^\nu(r) g_{SOt}^\nu(r) F_{qFt1}^\nu(r) \\ &+ \frac{2}{3} [g_{SOt}^\nu(r)]^2 F_{bFt1}^\nu(r), \end{aligned} \quad (3.12b)$$

where

$$\begin{aligned}
 F_{\text{bF}ts}^\nu(r_{12}) &= \Omega^2 \sum_{\text{isospin}} \sum_{\text{spin}} \int \Phi_{\text{F}}^\dagger(x_1, \dots, x_N) |\mathbf{L}_{12}|^4 P_{ts12}^\nu \Phi_{\text{F}}(x_1, \dots, x_N) d\mathbf{r}_3 \cdots d\mathbf{r}_N \\
 &= \frac{w_t^\nu(2s+1)}{4} \left[\frac{(z_1)^4 + (z_2)^4}{70} + \frac{(z_1 z_2)^2}{25} + \frac{(z_1)^2 + (z_2)^2}{5} \right. \\
 &\quad \left. - (-1)^{t+s} 9 \left\{ j_2(z_1) j_2(z_2) - j_1(z_1) j_1(z_2) \right. \right. \\
 &\quad \left. \left. + \frac{1}{6} [l(z_1) j_2(z_2) + l(z_2) j_2(z_1)] \right\} \right]. \tag{3.13}
 \end{aligned}$$

The choice of z_1 and z_2 in Eq. (3.13) is the same as in the case of Eq. (3.10).

Next, we consider the three-body cluster terms in relation to the necessary conditions on the spin-isospin-dependent structure functions.⁸⁾ More precisely, we properly take into account the three-body-cluster direct term originating from H_{ijk} that is of lowest order in the correlations, $h_{\text{C}ts}^\nu(r) \equiv f_{\text{C}ts}^\nu(r) - 1$. Here, H_{ijk} represents the terms with the two ∇_i operators in the kinetic energy operating on two different correlation functions, f_{ij} and f_{ik} .¹²⁾ Here, this three-body cluster term is expressed in terms of $h_{\text{C}ts}^\nu(r)$, but it is more convenient to express it approximately in terms of structure functions as explained in the following. The spin-isospin-dependent structure functions are defined as the Fourier transforms of $F_{ts}^\nu(r)$:

$$S_{ts}^\nu(k) = \rho \int [F_{ts}^\nu(r) - F_{ts}^\nu(\infty)] \exp(i\mathbf{k} \cdot \mathbf{r}) d\mathbf{r}. \tag{3.14}$$

If we keep only the lowest-order terms in $h_{\text{C}ts}^\nu(r)$, and temporarily disregard the exchange part on the right-hand side of Eq. (3.14), then we obtain the relation between $h_{\text{C}ts}^\nu(r)$ and $S_{ts}^\nu(k)$ as

$$h_{\text{C}ts}^\nu(r) \approx \frac{1}{4(2s+1)\pi^3 \rho w_t^\nu} \int S_{ts}^\nu(k) \exp(-i\mathbf{k} \cdot \mathbf{r}) d\mathbf{k}. \tag{3.15}$$

Using this relation, the above three-body cluster term composed of only $h_{\text{C}ts}^\nu(r)$ is written as

$$\frac{\langle H \rangle_{3d}}{N} \approx \frac{E_{3d}}{N} = -\frac{\hbar^2}{16\pi^2 m \rho} \sum_{n=1}^8 \int_0^\infty b_{cn} [S_{\text{C}pn}(k) - 1]^3 k^4 dk, \tag{3.16}$$

with $(b_{c1}, b_{c2}, b_{c3}, b_{c4}, b_{c5}, b_{c6}, b_{c7}, b_{c8}) = (1, 1, \xi/\eta, \eta/\xi, 3, 3, 3\xi/\eta, 3\eta/\xi)$. Here, we have

$$\begin{aligned}
 \left. \begin{aligned} S_{\text{cp}1}(k) \\ S_{\text{cp}2}(k) \end{aligned} \right\} &= 1 + \frac{T_{\text{a}1}^+(k)}{2\xi} + \frac{T_{\text{a}1}^-(k)}{2\eta} \\
 &\mp \frac{1}{2} \sqrt{\left(\frac{T_{\text{a}1}^+(k)}{\xi} - \frac{T_{\text{a}1}^-(k)}{\eta} \right)^2 + \frac{(T_{\text{a}1}^0(k) + T_{\text{a}0}^0(k))^2}{\xi\eta}} \geq 0, \tag{3.17a}
 \end{aligned}$$

$$\left. \begin{matrix} S_{\text{cp}3}(k) \\ S_{\text{cp}4}(k) \end{matrix} \right\} = 1 + \left(\frac{\frac{1}{2\xi}}{\frac{1}{2\eta}} \right) [T_{\text{a}1}^0(k) - T_{\text{a}0}^0(k)] \geq 0, \quad (3.17b)$$

$$\left. \begin{matrix} S_{\text{cp}5}(k) \\ S_{\text{cp}6}(k) \end{matrix} \right\} = 1 + \frac{T_{\text{b}1}^+(k)}{2\xi} + \frac{T_{\text{b}1}^-(k)}{2\eta} \\ \mp \frac{1}{2} \sqrt{\left(\frac{T_{\text{b}1}^+(k)}{\xi} - \frac{T_{\text{b}1}^-(k)}{\eta} \right)^2 + \frac{(T_{\text{b}1}^0(k) + T_{\text{b}0}^0(k))^2}{\xi\eta}} \geq 0, \quad (3.17c)$$

$$\left. \begin{matrix} S_{\text{cp}7}(k) \\ S_{\text{cp}8}(k) \end{matrix} \right\} = 1 + \left(\frac{\frac{1}{2\xi}}{\frac{1}{2\eta}} \right) [T_{\text{b}1}^0(k) - T_{\text{b}0}^0(k)] \geq 0, \quad (3.17d)$$

with

$$T_{\text{at}}^\nu(k) = S_{t1}^\nu(k) + S_{t0}^\nu(k), \quad (3.18a)$$

$$T_{\text{bt}}^\nu(k) = \frac{S_{t1}^\nu(k)}{3} - S_{t0}^\nu(k). \quad (3.18b)$$

The nonnegativities of the structure functions $S_{\text{cp}n}(k)$ ($n = 1 - 8$) given in (3.17) are obtained from the general form,

$$S_{\text{cp}n}(k) \equiv \frac{c_n}{N} \left\langle \left[\sum_{j=1}^N \boldsymbol{\omega}_{nj}^\dagger \exp(-i\mathbf{k} \cdot \mathbf{r}_j) \right] \cdot \left[\sum_{i=1}^N \boldsymbol{\omega}_{ni} \exp(i\mathbf{k} \cdot \mathbf{r}_i) \right] \right\rangle \geq 0, \quad (3.19)$$

where c_n is an appropriate normalization factor, and the operator $\boldsymbol{\omega}$ is chosen as

$$\frac{\mu_p}{\sqrt{\xi}} \frac{1 + \tau_z}{2} + \frac{\mu_n}{\sqrt{\eta}} \frac{1 - \tau_z}{2}, \frac{\tau_x \pm i\tau_y}{\sqrt{2}}, \left(\frac{\mu_p}{\sqrt{\xi}} \frac{1 + \tau_z}{2} + \frac{\mu_n}{\sqrt{\eta}} \frac{1 - \tau_z}{2} \right) \boldsymbol{\sigma}, \\ \text{and } \left(\frac{\tau_x \pm i\tau_y}{\sqrt{2}} \right) \boldsymbol{\sigma}. \quad (3.20)$$

It should be noted that when the operator $\boldsymbol{\omega}$ includes the parameters μ_p and μ_n , the extremes, corresponding to the strongest and weakest conditions, are evaluated under the condition $\mu_p^2 + \mu_n^2 = 1$, and this yields (3.17).

Next, taking into account the exchange correction and introducing denominators,⁸⁾ we modify and improve Eq. (3.16) as

$$\frac{E_3}{N}(\rho, \zeta) = -\frac{\hbar^2}{16\pi^2 m \rho} \sum_{n=1}^8 \int_0^\infty b_{cn} \frac{[S_{\text{cp}n}(k) - 1][S_{\text{cp}n}(k) - S_{\text{fn}}(k)]^2}{S_{\text{cp}n}(k)/S_{\text{fn}}(k)} k^4 dk \\ + \frac{E_{3\text{-corr}}}{N}(\rho, \zeta). \quad (3.21)$$

Here, we have $S_{\text{fn}}(k) = S_{\text{cpFn}}(k)$ [$S_{\text{cpFn}}(k)$ is $S_{\text{cp}n}(k)$ for the degenerate Fermi gas] for $n = 3, 4, 7$ and 8 , whereas

$$S_{\text{f}1}(k) = S_{\text{f}2}(k) = S_{\text{f}5}(k) = S_{\text{f}6}(k) = \xi S_{\text{cF}}^+(k) + \eta S_{\text{cF}}^-(k) \equiv S_{\text{f}}(k), \\ (n = 1, 2, 5 \text{ and } 6) \quad (3.22)$$

with

$$S_{\text{cF}}^+(k) \equiv 1 + \frac{(S_{\text{F11}}^+(k) + S_{\text{F10}}^+(k))}{\xi} = 1 + \frac{2S_{\text{F11}}^+(k)}{3\xi}, \quad (3\cdot23a)$$

$$S_{\text{cF}}^-(k) \equiv 1 + \frac{(S_{\text{F11}}^-(k) + S_{\text{F10}}^-(k))}{\eta} = 1 + \frac{2S_{\text{F11}}^-(k)}{3\eta}, \quad (3\cdot23b)$$

where $S_{\text{Fts}}^\nu(k)$ is $S_{ts}^\nu(k)$ for the degenerate Fermi gas. The relations between $S_{\text{cpFn}}(k)$ and $S_{\text{cF}}^\pm(k)$ are

$$S_{\text{cpF1}}(k) = S_{\text{cpF5}}(k) = \begin{cases} S_{\text{cF}}^+(k) & \text{for } \xi \geq \eta, \\ S_{\text{cF}}^-(k) & \text{for } \xi \leq \eta, \end{cases} \quad (3\cdot24a)$$

$$S_{\text{cpF2}}(k) = S_{\text{cpF6}}(k) = \begin{cases} S_{\text{cF}}^-(k) & \text{for } \xi \geq \eta, \\ S_{\text{cF}}^+(k) & \text{for } \xi \leq \eta, \end{cases} \quad (3\cdot24b)$$

The last term, $E_{3\text{-corr}}(\rho, \zeta)/N$, in Eq. (3·21) is introduced in order to make $E_3(\rho, \zeta)/N$ second or higher order in the correlation $[S_{ts}^\nu(k) - S_{\text{Fts}}^\nu(k)]$, and also in order to correctly take into account the second-order (i.e., lowest order) three-body-cluster two-particle-exchange terms that are composed of only $h_{\text{Cts}}^\nu(r)$ caused by H_{ijk} . Explicitly, it is given by

$$\begin{aligned} \frac{E_{3\text{-corr}}}{N}(\rho, \zeta) = & \frac{\hbar^2}{16\pi^2 m \rho} \int_0^\infty \left[W_0(k) + \frac{W_1^+(k)}{\xi} [S_{11}^+(k) - S_{10}^+(k) - S_{\text{F11}}^+(k) + S_{\text{F10}}^+(k)] \right. \\ & + \frac{W_1^-(k)}{\eta} [S_{11}^-(k) - S_{10}^-(k) - S_{\text{F11}}^-(k) + S_{\text{F10}}^-(k)] \\ & - W_2^+(k) \left\{ \frac{[S_{\text{c1}}^+(k) - S_{\text{cF}}^+(k)]^2}{S_{\text{c1}}^+(k)/S_{\text{cF}}^+(k)} + 3 \frac{[S_{\text{c2}}^+(k) - S_{\text{cF}}^+(k)]^2}{S_{\text{c2}}^+(k)/S_{\text{cF}}^+(k)} \right\} \\ & - W_2^-(k) \left\{ \frac{[S_{\text{c1}}^-(k) - S_{\text{cF}}^-(k)]^2}{S_{\text{c1}}^-(k)/S_{\text{cF}}^-(k)} + 3 \frac{[S_{\text{c2}}^-(k) - S_{\text{cF}}^-(k)]^2}{S_{\text{c2}}^-(k)/S_{\text{cF}}^-(k)} \right\} \\ & \left. - \frac{W_2^0(k)}{\xi\eta} \left\{ \frac{[S_{11}^0(k) + S_{01}^0(k)]^2}{3} + [S_{10}^0(k) + S_{00}^0(k)]^2 \right\} \right] k^4 dk, \quad (3\cdot25) \end{aligned}$$

with

$$W_0(k) = 4 \left\{ \frac{[S_{\text{cF}}^+(k) - 1] [S_{\text{cF}}^+(k) - S_{\text{f}}(k)]^2}{S_{\text{cF}}^+(k)/S_{\text{f}}(k)} + \frac{[S_{\text{cF}}^-(k) - 1] [S_{\text{cF}}^-(k) - S_{\text{f}}(k)]^2}{S_{\text{cF}}^-(k)/S_{\text{f}}(k)} \right\}, \quad (3\cdot26a)$$

$$W_1^\pm(k) = 2 \frac{S_{\text{f}}(k) [S_{\text{cF}}^\pm(k) - S_{\text{f}}(k)]}{[S_{\text{cF}}^\pm(k)]^2} \left\{ 2 [S_{\text{cF}}^\pm(k)]^2 - S_{\text{cF}}^\pm(k) - S_{\text{f}}(k) \right\}, \quad (3\cdot26b)$$

$$W_2^\pm(k) = 4 \left\{ S_{\text{cF}}^\pm(k) - 1 - S_{\text{f}}(k) + \left[\frac{S_{\text{f}}(k)}{S_{\text{cF}}^\pm(k)} \right]^3 \right\}, \quad (3\cdot26c)$$

$$W_2^0(k) = S_{\text{cF}}^+(k) + S_{\text{cF}}^-(k) - 2 - S_f(k) \left\{ 2 - \left[\frac{S_f(k)}{S_{\text{cF}}^+(k)S_{\text{cF}}^-(k)} \right]^2 [S_{\text{cF}}^+(k) + S_{\text{cF}}^-(k)] \right\}. \quad (3\cdot26d)$$

Furthermore, the functions $S_{cn}^\pm(k)$ ($n = 1, 2$) are defined as

$$S_{c1}^+(k) \equiv 1 + \frac{T_{a1}^+(k)}{\xi} \geq 0, \quad (3\cdot27a)$$

$$S_{c1}^-(k) \equiv 1 + \frac{T_{a1}^-(k)}{\eta} \geq 0, \quad (3\cdot27b)$$

$$S_{c2}^+(k) \equiv 1 + \frac{T_{b1}^+(k)}{\xi} \geq 0, \quad (3\cdot27c)$$

$$S_{c2}^-(k) \equiv 1 + \frac{T_{b1}^-(k)}{\eta} \geq 0. \quad (3\cdot27d)$$

These inequalities for $S_{cn}^\pm(k)$ are easily proved as in the case of (2.6). Also, in the case of the degenerate Fermi gas, $S_{cn}^\pm(k)$ reduces to $S_{\text{cF}}^\pm(k)$ defined by Eq. (3.23), irrespective of the value of n . Note that, in the integrand of Eq. (3.25), the fourth and fifth terms have denominators corresponding to the modification in §2.

Combining the above results, the approximate energy expression for asymmetric nuclear matter is obtained at this point as

$$\frac{E}{N}(\rho, \zeta) = \frac{E_2}{N}(\rho, \zeta) + \frac{E_3}{N}(\rho, \zeta). \quad (3\cdot28)$$

This expression satisfies the following conditions (i) – (vi), similarly to the case of partially spin-polarized matter:

(i) $E(\rho, \zeta)/N$ is expressed as a functional of the spin-isospin-dependent radial distribution functions, $F_{ts}^\nu(r)$, tensor distribution functions, $F_{Tt}^\nu(r)$, and spin-orbit distribution functions, $F_{\text{SO}t}^\nu(r)$, defined by Eq. (3.5).

(ii) $E(\rho, \zeta)/N$ has features similar to those of the corresponding quantities for neutron matter, $E_{\text{neu}}(\rho)/N$, and symmetric nuclear matter, $E_{\text{sym}}(\rho)/N$, whose explicit expressions are given in Refs. 7) and 13). These features are described in the following.

(iia) The central, tensor and spin-orbit components of the potential energies are expressed exactly, whereas the quadratic orbital angular momentum part and the quadratic spin-orbit part of the potential energies are expressed so as to include at least the two-body cluster terms.

(iib) The one-body and two-body cluster terms of the kinetic energy are included in the expression. Also included are the lowest-order direct and two-particle-exchange three-body-cluster terms that are composed of only $h_{\text{C}ts}^\nu(r)$ arising from H_{ijk} . Other cluster terms are partially included.

(iic) The necessary conditions on the spin-isospin-dependent structure functions $S_{\text{c}pn}(k)$ are guaranteed.

(iii) $E(\rho, \zeta)/N$ is symmetric with respect to exchange of ξ and η .

(iv) $E(\rho, \zeta)/N$ reduces to the expressions previously obtained in the limiting cases: $E(\rho, \zeta = 0)/N = E_{\text{sym}}(\rho)/N$ and $E/N(\rho, \zeta = 1)/N = E_{\text{neu}}(\rho)/N$.

(v) $E(\rho, \zeta)/N$ is a smooth function of ζ , and thus,

$$\left. \frac{\partial E(\rho, \zeta)/N}{\partial \zeta} \right|_{\zeta=0} = 0. \quad (3.29)$$

(vi) The kinetic energy terms caused by the correlation between particles are of second or higher order in the correlation.

3.2. Phenomenological additional terms

In this subsection, we consider a phenomenological modification of the energy expression with the purpose of obtaining reasonable values of the energy per nucleon. This is done because the variational calculations without such a modification give energies that are too low, with unrealistically long tails of the noncentral distribution functions. The modification for the case of symmetric nuclear matter and neutron matter is proposed in Refs. 7) and 13), and it is fairly successful. In this subsection, we make a similar modification for asymmetric nuclear matter.

The modification is made by adding phenomenological noncentral correction terms to the original energy expression, Eq. (3.28). The form of the added term is

$$\begin{aligned} \frac{E_m}{N} = & -2\pi\rho \sum_{t=0}^1 \sum_{\nu} \int_0^{\infty} [1 - D(r_0; r)] \left\{ F_{Tt}^{\nu}(r) V_{Tt}(r) + F_{SOt}^{\nu}(r) V_{SOt}(r) \right. \\ & \left. + \left[F_{qSOt}^{\nu}(r) - \frac{2}{3} F_{qLt1}^{\nu}(r) \right] V_{qSOt}(r) \right\} r^2 dr, \end{aligned} \quad (3.30)$$

where $r_0 = (3/4\pi\rho)^{1/3}$ is the radius of a sphere of volume $1/\rho$. The explicit form of the damping function $D(r_0; r)$ in Eq. (3.30) is chosen as

$$D(r_0; r) = \exp \left[- \left(\frac{r}{ar_0} \right)^2 \right], \quad (3.31)$$

with an adjustable parameter a , whose value is determined so that the saturation point of symmetric nuclear matter obtained by the calculation is close to the empirical one.

In practice, the introduction of E_m/N implies that purely noncentral components of the two-body nuclear potential are multiplied by $D(r_0; r)$, so that the noncentral potentials are damped as the two nucleons move away from each other. In the case of the $(\mathbf{s} \cdot \mathbf{L})^2$ part of the nuclear potential implicitly composed of the central and purely noncentral components, only the latter component is multiplied by $D(r_0; r)$.

As a result of this modification, the calculations give relatively reasonable saturation point, but the fit is not quite satisfactory: Either the obtained saturation density is somewhat higher than the empirical one, or the saturation energy is higher than the empirical value, or both. For example, if the isoscalar part of the AV18 potential is used with the damping function $D(r_0; r)$, the saturation energy for symmetric nuclear matter is $E_{\text{sat}}/N = -15.78$ MeV, with the saturation density $\rho_{\text{sat}} = 0.195$ fm $^{-3}$

for $a = 1.45$. This deviation from the empirical saturation point is similar to the deviation found with various other non-relativistic many-body calculations, i.e., the theoretical saturation points lie on the so-called Coester band. Actually, the above-mentioned saturation point is in the boundary region of the Coester band on the side nearer the empirical saturation point. Because the deviation is possibly caused by the lack of three-body nuclear forces, in this study, we take into account the contribution of additional three-body interactions (TNI) by following the method employed by Lagaris and Pandharipande,¹⁴⁾ as described below.

The isoscalar part of the AV18 potential V_{ij} is expressed as the sum of 14 two-body operators O_{ij}^p times their radial dependence composed of the one-pion-exchange long-range part V_p^π , the intermediate part V_p^I , and the short-range repulsive part V_p^R . The TNI is separated into two parts, a repulsive part (TNR) and an attractive part (TNA). Then, the effect of the TNR is incorporated into the two-body nuclear potential as a reduction of the intermediate-range parts of the two-body forces:

$$V_{ij} + \text{TNR} = \sum_{p=1}^{14} [V_p^\pi(r_{ij}) + V_p^I(r_{ij})e^{-\gamma\rho} + V_p^R(r_{ij})] O_{ij}^p, \quad (3.32)$$

where the reduction factor $\exp[-\gamma\rho]$ includes an adjustable parameter γ . The TNA is taken into account simply by the additional energy

$$\frac{E_{\text{TNA}}}{N} = \beta\rho^2 e^{-\delta\rho} (3 - 2\zeta^2), \quad (3.33)$$

where β and δ are adjustable parameters. Then, the total energy is expressed as the sum of Eqs. (3.28), (3.30) and (3.33) with the interaction Eq. (3.32).

3.3. Results of numerical calculations

As mentioned in the last subsection, we employ the modified isoscalar part of the AV18 potential. In the last subsection, four adjustable parameters, a , γ , β and δ , were introduced. Among them, we assume $\gamma = 0.15 \text{ fm}^3$,^{14),15)} and the remaining three parameters are determined so as to reproduce the empirical saturation point for symmetric nuclear matter. The values of the parameters so chosen are $a = 1.4$, $\beta = -265 \text{ MeVfm}^6$ and $\delta = 4.4 \text{ fm}^3$, giving the saturation density $\rho_{\text{sat}} = 0.16 \text{ fm}^{-3}$, the saturation energy $E_{\text{sat}}/N = -15.80 \text{ MeV}$ and the incompressibility $K = 232 \text{ MeV}$. By the way, if we interpolate between the energies for symmetric nuclear matter ($\zeta = 0$) and neutron matter ($\zeta = 1$) using a quadratic form in ζ , then the symmetry energy (the coefficient of ζ^2) is evaluated to be 29.38 MeV . Once the values of the adjustable parameters are fixed, the EL equations for the actual variational functions $F_{Cts}^\nu(r)$, $g_{Tt}^\nu(r)$ and $g_{S0t}^\nu(r)$ (consisting of 16 coupled integrodifferential equations) are solved numerically for asymmetric nuclear matter. The results for the energy are plotted in Figs. 5 and 6, and detailed discussion of them is given in §4.

The various distribution functions and the nonnegative structure functions are displayed in Figs. 7 – 12 for $\rho = 0.16 \text{ fm}^{-3}$, $\zeta = 0.2$ and 0.8 . The central distribution functions shown in Figs. 7 and 8 have two features, the effect of the exclusion principle, or more exactly, of the antisymmetrization of the wave function, and the

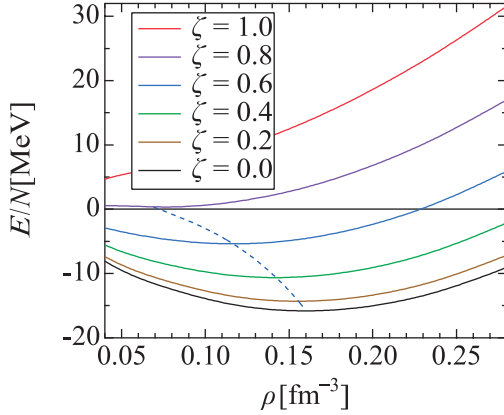


Fig. 5. Energies per particle, E/N , for asymmetric nuclear matter as functions of the number density ρ with the degree of asymmetry $\zeta = 0, 0.2, 0.4, 0.6, 0.8$, and 1. The dotted curve connects the minimum points of the solid curves.

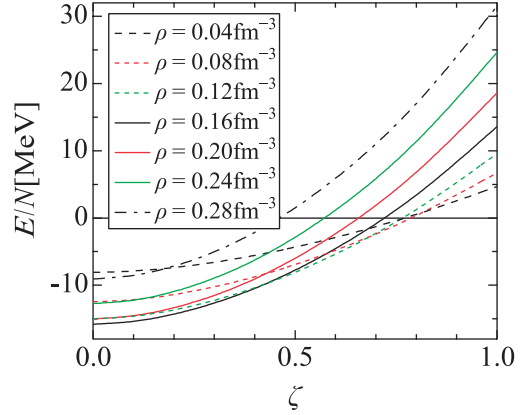


Fig. 6. Energies per particle, E/N , for asymmetric nuclear matter as functions of the degree of asymmetry, ζ .

influence of the nuclear force. More precisely, except for the dips around the origin due to the strong repulsive core, the spatially odd states [$F_{11}^\nu(r)$ and $F_{00}^0(r)$] are pushed out from the origin more than the even states [$F_{10}^\nu(r)$ and $F_{01}^0(r)$], which is an effect of antisymmetrization, and the distribution functions of the even states have high peaks around $r = 1$ fm, reflecting the strong attractive forces. When the distribution functions for $\zeta = 0.2$ and $\zeta = 0.8$ are compared with each other, the shapes are found to be similar, except for their absolute values. According to the general rule for the ground state, the noncentral distribution functions plotted in Figs. 9 and 10 always take values (including the signs) that lower the total energy. The conspicuous noncentral distributions are the tensor distribution function for the triplet-even state, $F_{T0}^0(r)$, and the spin-orbit distribution function for the triplet-odd states $F_{SO1}^\nu(r)$, in particular $F_{SO1}^-(r)$ for the case of large asymmetry ($\zeta = 0.8$).

Regarding the structure functions, we first note the behavior of $S_{cn}^\pm(k)$ [Eq. (3-27)] displayed in Figs. 11 and 12. It is seen that as k approaches zero, the quantities $S_{c1}^\pm(k)$ increase to infinity, while $S_{c2}^\pm(k)$ tend to zero. Therefore, according to Eqs. (3-27) and (3-18), the quantities $S_{11}^\pm(k) + S_{10}^\pm(k)$ increase to infinity as k goes to zero, while $S_{11}^\pm(k)/3 - S_{10}^\pm(k)$ do not. This means that both $S_{11}^\pm(k)$ and $S_{10}^\pm(k)$ increase to infinity as k approaches zero. This kind of increase is likely to be a sign of nucleon pairing;^{*)} it is seen, in this case, in the triplet-odd state and singlet-even state. From the figures, it is also seen that there are minima in the curves of $S_{c1}^\pm(k)$. When the asymmetry is not large (Fig. 11), the minima of the two curves appear at values of k that do not differ greatly. By contrast, when the asymmetry is large

^{*)} Because our formulation does not take into account the nucleon pairing explicitly, the existence of this pairing is not proved but only suggested by the infinite increase of the structure function as $k \rightarrow 0$, which implies a positive (attractive) long-ranged spatial correlation in the corresponding pair distribution function.

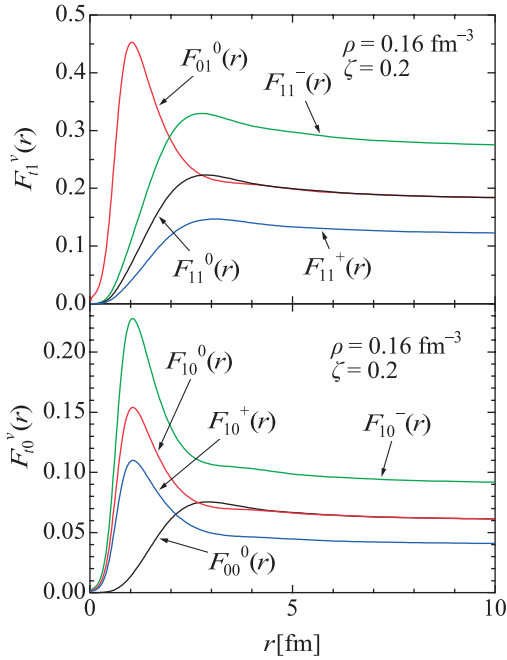


Fig. 7. Radial distribution functions $F_{l1}^{\nu}(r)$ for asymmetric nuclear matter at $\rho = 0.16 \text{ fm}^{-3}$, $\zeta = 0.2$.

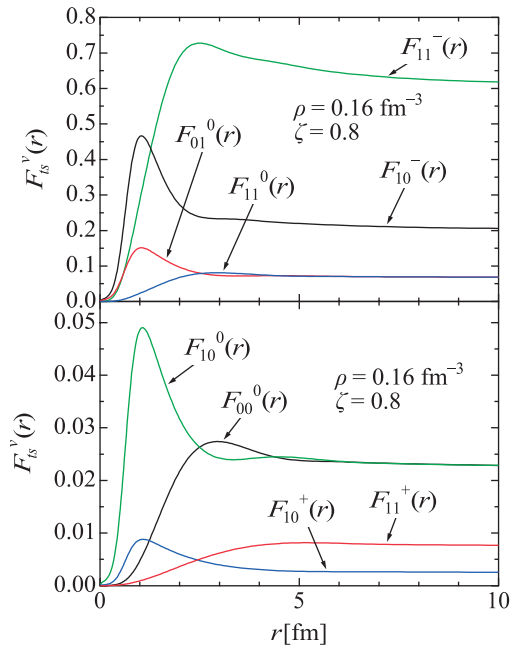


Fig. 8. Radial distribution functions $F_{ls}^{\nu}(r)$ for asymmetric nuclear matter at $\rho = 0.16 \text{ fm}^{-3}$, $\zeta = 0.8$.

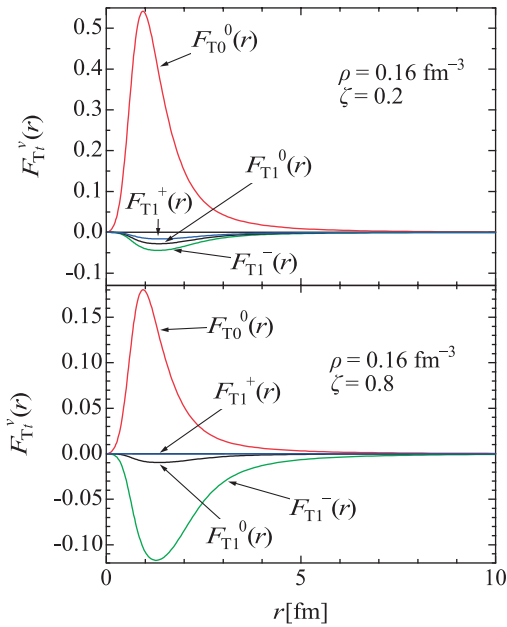


Fig. 9. Tensor distribution functions $F_{Tl}^{\nu}(r)$ for asymmetric nuclear matter at $\rho = 0.16 \text{ fm}^{-3}$, $\zeta = 0.2$, and 0.8 .

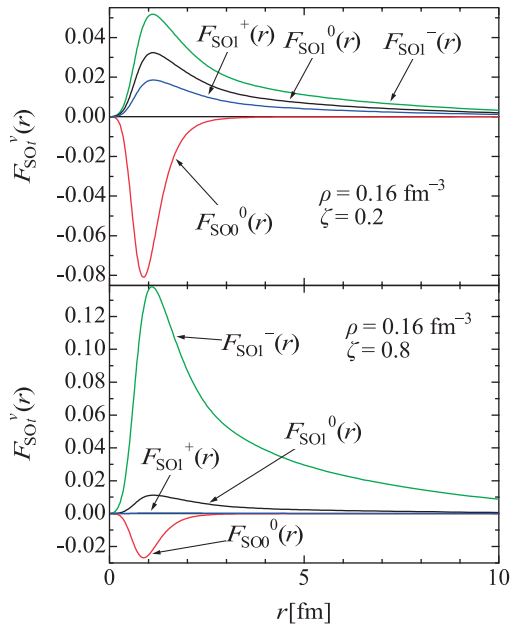


Fig. 10. Spin-orbit distribution functions $F_{SOlt}^{\nu}(r)$ for asymmetric nuclear matter at $\rho = 0.16 \text{ fm}^{-3}$, $\zeta = 0.2$, and 0.8 .

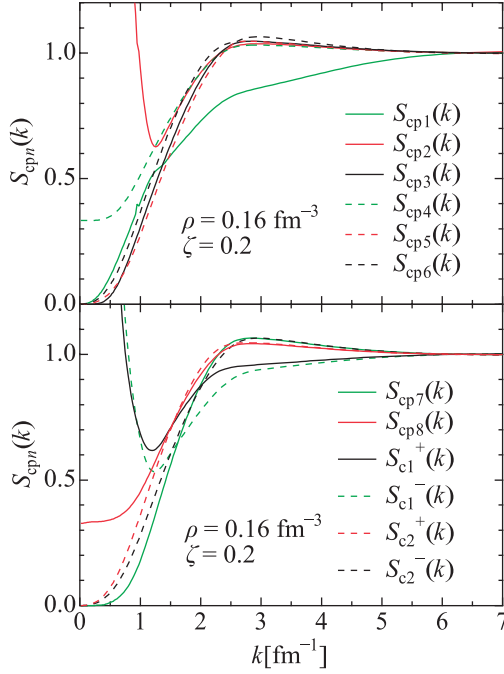


Fig. 11. Structure functions $S_{cpn}(k)$ and $S_{cn}^{\pm}(k)$ for asymmetric nuclear matter at $\rho = 0.16 \text{ fm}^{-3}$, $\zeta = 0.2$.

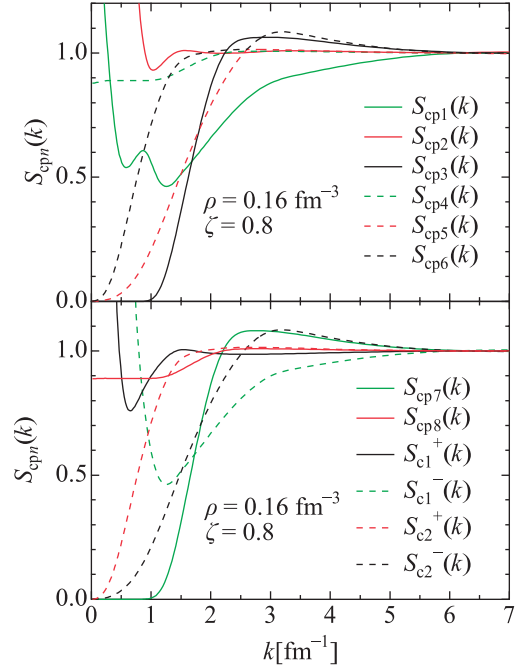


Fig. 12. Structure functions $S_{cpn}(k)$ and $S_{cn}^{\pm}(k)$ for asymmetric nuclear matter at $\rho = 0.16 \text{ fm}^{-3}$, $\zeta = 0.8$.

(Fig. 12), the minimum of $S_{c1}^{-}(k)$ appears at a significantly larger value of k than the minimum of $S_{c1}^{+}(k)$. In this case, the neutron density is considerably higher than the proton density, and, accordingly, two neutrons come nearer to each other than do two protons. This smaller value of r corresponds to a larger value of k , and this explains the difference between the positions of the two minimum points. The square root of Eq. (3·17a) and the difference between the values of k at the minimum points of $S_{c1}^{\pm}(k)$ result in the wavy behavior of $S_{cp1}(k)$.

§4. New term in the mass formula

4.1. Impossibility of expanding the energy as a power series in $(\rho_n - \rho_p)^2/\rho^2$

In the last section, we obtained values of the energy per particle $E(\rho, \zeta)/N$ for various values of ρ and ζ . Now we closely examine these values, in particular, the ζ dependence of $E(\rho, \zeta)/N$. For this purpose, we define $E_{a-s}(\rho, \zeta)/N$ as

$$\frac{E_{a-s}}{N}(\rho, \zeta) = \frac{E}{N}(\rho, \zeta) - \frac{E}{N}(\rho, 0). \quad (4.1)$$

It has been widely assumed or, rather, believed that E_{a-s}/N of infinite nuclear matter can be expanded as a power series in ζ^2 . However, if the results plotted in Figs. 6 and 13 are closely inspected, the possibility of a power series expansion seems doubtful.

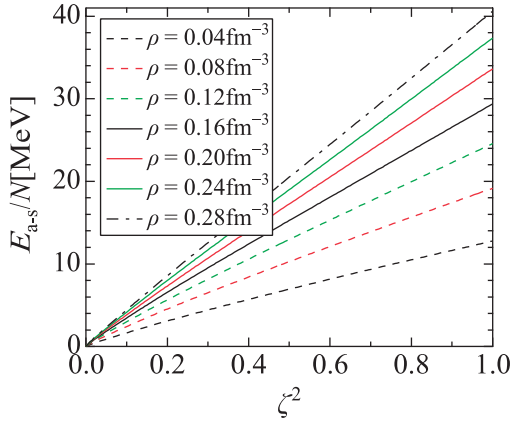


Fig. 13. Energy difference per particle $E_{a-s}(\rho, \zeta)/N$ [Eq. (4.1)] for asymmetric nuclear matter as functions of ζ^2 .

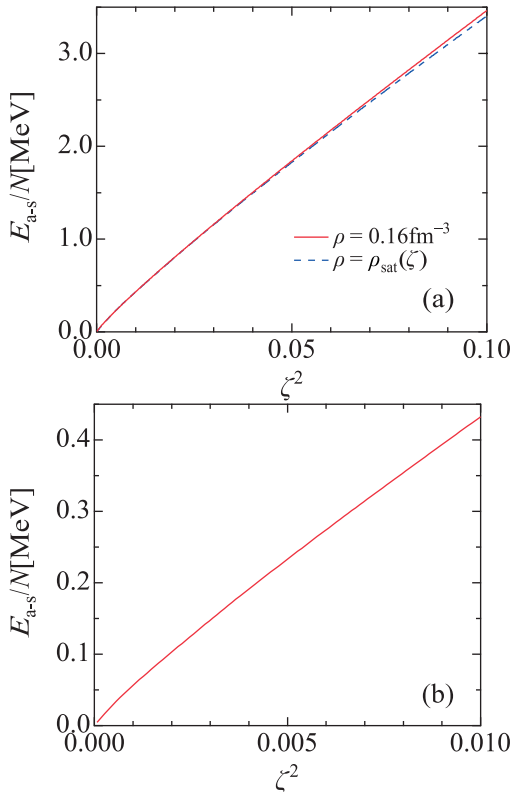


Fig. 14. Energy difference per particle $E_{a-s}(\rho, \zeta)/N$ for asymmetric nuclear matter as functions of ζ^2 : (a) $\zeta^2 \leq 0.1$; (b) $\zeta^2 \leq 0.01$. The solid curve represents $E_{a-s}(\rho, \zeta)/N$ at $\rho = 0.16 \text{ fm}^{-3}$, while the dashed curve represents $E_{as-s}(\zeta)/N$ defined in §4.2.

In particular, the curves in Fig. 6 near $\zeta = 0$ seem to deviate from the expected ζ^2 -dependence.

In order to clarify the situation, we plot E_{a-s}/N with the abscissa taken as ζ^2 in Fig. 13, and for the normal density, $\rho = 0.16 \text{ fm}^{-3}$, two magnified graphs of the same quantity in the neighborhood of $\zeta^2 = 0$ are given in Fig. 14. If the power series expansion were valid, the curves for E_{a-s}/N would approach lines as the graphs are limited within a narrower range of values of ζ . However, it is found that the actual situation is the reverse: The curve in the narrowest region near $\zeta^2 = 0$ (Fig. 14(b)) deviates most from a line.

For further confirmation of the impossibility of a power series expansion, here we attempt to carry out an expansion. We attempt to compute with three terms, up to ζ^6 . (For E_{a-s}/N , the constant term vanishes.) It is found that the coefficients depend strongly on the region of ζ^2 that we attempt to fit. Furthermore, when we consider the region in the neighborhood of $\zeta^2 = 0$, the coefficients of the ζ^4 and ζ^6 terms are absurdly large, and if we use such a series in the region of larger ζ^2 , the series deviates greatly from the true E_{a-s}/N . We have also confirmed that, even if we include the ζ^8 and ζ^{10} terms, no appreciable improvement of the fit is obtained.

It is important to note that the impossibility of the expansion is not caused by the complexity of the approximate energy expression given in §3. The tendency for deviation from the ζ^2 law near $\zeta = 0$ was already seen in our calculations of hypothetical nuclear matter, in which nucleons are assumed to interact with each other through central forces, such as the OMY potential, as in Ref. 16). In that case, nuclear matter

was treated without consideration of the noncentral nuclear forces, and, accordingly, the effective theory described in §3.2 of this paper was not necessary.

The impossibility of a power series expansion in ζ^2 is neither a spurious artifact of the complicated integrodifferential equations nor a characteristic peculiar to isospin polarization. To show this, in the appendix we present results of a study of fictitious spin-polarized neutron matter for which the nuclear force is varied somewhat arbitrarily. In that case, the Euler-Lagrange equations are a much simpler set of integrodifferential equations than the set for asymmetric nuclear matter. In the appendix, the energy per neutron $E(\rho, \kappa)/N$ is calculated at various values of the number density ρ and the degree of polarization $\kappa = (\rho_u - \rho_d)/\rho$. (Here, ρ_u and ρ_d are the number densities of spin-up and spin-down neutrons, respectively.) Then, the behavior of the difference between the energies of polarized matter and unpolarized matter,

$$\frac{E_{\text{pol}}}{N}(\rho, \kappa) = \frac{E}{N}(\rho, \kappa) - \frac{E}{N}(\rho, 0), \quad (4.2)$$

is compared with the behavior of $E_{a-s}(\rho, \zeta)/N$ obtained above. This comparison shows that, for some neutron-neutron potentials, these two functions are very similar, and in particular, $E_{\text{pol}}(\rho, \kappa)/N$ cannot be expanded as a power series in κ^2 .

4.2. A new term suggesting the partial formation of clusters

As the unfeasibility of a power series expansion of E_{a-s}/N in ζ^2 has become clear, our next problem is to find a formula to represent E_{a-s}/N . The main property of E_{a-s}/N which makes impossible its expansion as a power series is the strong dependence of the gradient $\partial[E_{a-s}/N]/\partial(\zeta^2)$ on ζ^2 in the neighborhood of $\zeta^2 = 0$. If we turn our attention to the mass formula of (finite) nuclei, we find a term having such a property. This term is called the Wigner term, and has the form $c_w |I|/(A + a_w)$,¹⁷⁾ where A is the mass number, and c_w and a_w are constants. (a_w is often taken to be zero.) I is the difference between the neutron number and the proton number, and the symmetry between neutrons and protons is maintained by taking the absolute value. The Wigner term is important for light nuclei, but its importance diminishes as A increases, because some other terms in the mass formula increase in proportion to A , whereas the Wigner term does not. For this reason, it has been assumed to this time that a term similar to the Wigner term, i.e., a term proportional to $|\zeta|$, does not exist for infinite nuclear matter. However, if such a term does exist, what would be the result? It is rather easy to see that if a $|\zeta|$ term is added to the power series in ζ^2 , the above-mentioned strong dependence of $\partial[E_{a-s}/N]/\partial(\zeta^2)$ on ζ^2 is reproduced in the region moderately near $\zeta^2 = 0$. However, in the region very close to $\zeta^2 = 0$, the reproduction is poor; when E_{a-s}/N is regarded as a function of ζ , not of ζ^2 , the result of our many-body calculation is smooth at $\zeta = 0$, while a function including a $|\zeta|$ term is not. This defect can be removed by replacing $|\zeta|$ by $(\zeta^2 + \zeta_0^2)^{1/2}$, with ζ_0 being a small number. Thus, our choice is

$$\frac{E}{N}(\rho, \zeta) = \varepsilon_0(\rho) + \frac{E_{a-s}}{N}(\rho, \zeta), \quad (4.3a)$$

with

$$\frac{E_{a-s}}{N}(\rho, \zeta) = \varepsilon_1(\rho) \left[\sqrt{\zeta^2 + \zeta_0^2} - \zeta_0 \right] + \sum_{n=1}^q \varepsilon_{2n}(\rho) \zeta^{2n}. \quad (4.3b)$$

The first term on the right-hand side of Eq. (4.3b) is the new term. If the number density ρ is given, then $\varepsilon_0, \varepsilon_1, \varepsilon_{2n}$ and ζ_0 are regarded as parameters, among which ε_0 is fixed by the result for symmetric nuclear matter. Although not indicated explicitly, ζ_0 also depends on ρ . The parameters $\varepsilon_1, \varepsilon_{2n}$ and ζ_0 are determined by comparison of the expression (4.3b) with the results of the many-body calculations for asymmetric nuclear matter. Using the expression (4.3b) with $q = 3$ (up to ζ^6), we obtain the results given in Table I. As expected, ζ_0 is very small, and this smallness explains the impossibility of a power series expansion: An expansion of $(\zeta^2 + \zeta_0^2)^{1/2}$ as a power series in ζ^2 converges only in a very narrow region, $|\zeta| \leq \zeta_0$, which is much narrower than the region of physical interest. The quantity ε_1 is not very large, but certainly it is non-zero. We also see that ε_2 , which is often regarded as the symmetry-energy coefficient, takes a reasonable value. The smallness of ε_4 and ε_6 shows that, even if we omit them, the $\varepsilon_2 \zeta^2$ term represents the general tendency of the energy of asymmetric nuclear matter fairly well. It should be emphasized that Eq. (4.3b) reproduces the results of many-body calculations very accurately. For example, at the saturation density $\rho = 0.16 \text{ fm}^{-3}$, we carried out many-body calculations at 28 values of $\zeta^2 (\neq 0)$, and these 28 data are reproduced by the 5 parameter formula Eq. (4.3b) within a deviation of 4 keV. This accuracy is one order of magnitude better than the accuracy obtained with the simple power series in ζ^2 . This improvement of the accuracy supports the appropriateness of the new term.

Now we consider the question of what kind of phenomenon could cause the appearance of the new term. We strongly suspect that the partial formation of clusters in nuclear matter is the main cause. Such clusters that are likely to be formed are light self-mirror nuclei. These nuclei have especially large binding energies compared with other isobars due to the Wigner term. The most probable clusters are ${}^2\text{H}$ and ${}^4\text{He}$, which are the only bound states among the isobars. For simplicity, let us consider ${}^2\text{H}$ only. Because a cluster is formed only when two nucleons approach each other closely, we consider a small region in nuclear matter and assume that there are N_p protons and N_n neutrons in this region. Then, the maximum number of ${}^2\text{H}$ clusters that can be formed in this region is the smaller of N_p and N_n , i.e.,

Table I. Values of the parameters in Eq. (4.3b). The last digit of each is uncertain.

$\rho[\text{fm}^{-3}]$	$\varepsilon_1[\text{MeV}]$	ζ_0	$\varepsilon_2[\text{MeV}]$	$\varepsilon_4[\text{MeV}]$	$\varepsilon_6[\text{MeV}]$
0.04	1.74	0.078	12.41	-1.72	0.46
0.08	2.15	0.063	19.00	-3.05	1.20
0.12	2.29	0.054	24.24	-3.43	1.59
0.16	2.32	0.048	28.63	-3.21	1.76
0.20	2.31	0.044	32.35	-2.65	1.72
0.24	2.26	0.041	35.60	-2.07	1.66
0.28	2.21	0.038	38.45	-1.55	1.59

$\min(N_n, N_p)$. If

$$(N_n - N_p) / (N_n + N_p) = \zeta, \quad (4.4a)$$

then

$$\min(N_n, N_p) = (1 - |\zeta|) (N_n + N_p) / 2. \quad (4.4b)$$

Thus, the absolute value $|\zeta|$ appears. Since cluster formation lowers the energy, the absolute value $|\zeta|$ would appear in the energy formula with a positive coefficient.

Actually, the above argument is over-simplified. First, formation of clusters does not generally occur to the maximum degree; on the contrary, it occurs with a rather low probability. Second, Eq. (4.4a) does not hold in general, although it will hold on average. Here, it should be noted that, due to the exclusion principle, the spatial distributions of protons and neutrons are much more uniform than the distribution of freely and randomly moving classical particles. Therefore, the deviation from Eq. (4.4a) is considerably smaller than that estimated from the distributions of classical particles of two kinds. The third simplification regards the choice of clusters; light nuclei (e.g., ${}^3\text{H}$ and ${}^3\text{He}$) other than self-mirror nuclei may be formed as clusters. If these simplifications are removed, the nonsmooth behavior of the energy expression caused by the presence of $|\zeta|$ will disappear, but in the region not very close to $\zeta = 0$, the general properties of the $|\zeta|$ term will remain. The above argument is one reason we suspect cluster formation to be the cause of the new term, and the results given in the appendix further support this conjecture.

The above argument is consistent with the behavior of the distribution functions. The large peaks of $F_{01}^0(r)$ around $r = 1$ fm seen in Figs. 7 and 8 together with the strong tensor correlation $F_{T0}^0(r)$ found in Fig. 9 indicate that the triplet-even state gives a large contribution to the binding energy, part of which may be through cluster formation. Note that ${}^2\text{H}$ is in the triplet-even state, and other nuclei regarded as possibilities for the cluster have large triplet-even components. It should also be noted that, as seen from comparison of Figs. 7 and 8, the weight of the triplet-even state decreases as ζ increases.

The finding of a new term in the energy expression for nuclear matter suggests that a corresponding term is necessary in the mass formula for finite nuclei. When we treat finite nuclei, we should plot the energy at the saturation density, $\rho_{\text{sat}}(\zeta)$, for each value of ζ , rather than the energy at the fixed saturation density, $\rho_{\text{sat}}(0)$, of symmetric nuclear matter. As ζ increases from zero, $\rho_{\text{sat}}(\zeta)$ remains very near $\rho_{\text{sat}}(0)$, until ζ becomes close to 0.1, and then it begins to decrease, as shown in Fig. 5. The energy per nucleon at $\rho_{\text{sat}}(\zeta)$ measured from that at $\zeta = 0$, $\rho = \rho_{\text{sat}}(0)$, which we denote by $E_{\text{as-s}}(\zeta)/N$, is plotted in Fig. 14(a) by the dashed curve in the region $\zeta^2 < 0.1$. In the region $\zeta^2 \ll 1$, this curve is very close to the solid curve representing $E_{\text{a-s}}(\rho_{\text{sat}}(0), \zeta)/N$. Although not shown in the figures, values of $E_{\text{as-s}}(\zeta)/N$ are obtained up to $\zeta \approx 0.8$, as seen in Fig. 5. A suitable expression for $E_{\text{as-s}}(\zeta)/N$ takes a form similar to Eq. (4.3b),

$$\frac{E_{\text{as-s}}}{N}(\rho, \zeta) = \varepsilon_{1s} \left[\sqrt{\zeta^2 + \zeta_{0s}^2} - \zeta_{0s} \right] + \sum_{n=1}^q \varepsilon_{2ns} \zeta^{2n}, \quad (4.5)$$

Table II. Values of the parameters in Eq. (4.5). The last row lists the values determined with the data in the limited range, $0 < \zeta \leq 0.3$. The last digit of each is uncertain.

q	$\varepsilon_{1s}[\text{MeV}]$	ζ_{0s}	$\varepsilon_{2s}[\text{MeV}]$	$\varepsilon_{4s}[\text{MeV}]$	$\varepsilon_{6s}[\text{MeV}]$
3	2.14	0.041	28.97	-8.58	-2.01
1	2.81	0.054	26.63	—	—

where ε_{1s} , ε_{2ns} , and ζ_{0s} are parameters independent of ρ , unlike the parameters in Eq. (4.3b). By taking powers of ζ^2 in Eq. (4.5) up to ζ^6 ($q = 3$), we compare Eq. (4.5) with the results of the variational calculations, and the parameter values obtained are given in Table II. The accuracy of the fit is good: The differences between the right-hand side of Eq. (4.5) and the results of the variational calculations are less than 3 keV. If we use a simple power series, omitting the first term on the right-hand side of Eq. (4.5) with $q = 3$, the fit is much worse, with the differences exceeding 80 keV at some values of ζ . Even if we increase the number of terms in the simple power series expansion up to five ($q = 5$), the differences exceed 23 keV, with ε_{2ns} being absurdly large.

If we regard a finite nucleus as a part of nuclear matter, the neutron excess divided by the mass number, I/A , corresponds to ζ . The nuclidic region $I/A \leq 0.3$ includes most known nuclides and many undiscovered nuclides. The existence of nuclides is also expected in the region $I/A > 0.3$, but these nuclei are likely to have neutron skins. Therefore, their inner parts, which can be regarded as parts of nuclear matter, will have fewer neutrons, and the corresponding ζ will be considerably smaller than I/A . In most nuclear mass formulas, no term including I^{2q} ($q > 1$) as a factor is used. From these considerations, we conclude that it is meaningful to compare the results of the variational calculations for $\zeta \leq 0.3$ with the right-hand side of Eq. (4.5) with $q = 1$. The parameter values obtained through this comparison are also given in Table II. With these parameters, the right-hand side of Eq. (4.5) represents the results of the variational calculations for $\zeta \leq 0.3$ within an accuracy of 4 keV.

For finite nuclei, the corresponding new term should be $b_1((I^2 + I_0^2)^{1/2} - I_0)$, where b_1 and I_0 are positive constants. If we consider the sensitivity of the results to nuclear forces, as demonstrated in the appendix, we believe that b_1 and I_0 should be treated as adjustable parameters. If I_0 is very small, this term has some similarity to the Wigner term, but it remains important in heavy nuclei. The coefficient b_1 may be rather small, but the effect of this new term should be clarified by future studies of the mass formula.

§5. Concluding remarks

In this paper we constructed an approximate energy expression for asymmetric nuclear matter. This expression is fairly complicated, but it is one of the simplest expressions in conformity with our guiding principle. There is ample room for improvement. For example, refinements of the kinetic energy expressions caused by noncentral correlations are expected to replace the phenomenological modification,

as in Eq. (3·30), and a direct treatment of the bare three-body nuclear force is desirable, in place of the phenomenological one used in this paper. It would be interesting to see whether the new term found in this paper remains after these improvements. It is also important to determine whether other calculational methods give a similar term and whether the interpretation that this new term is due to cluster formation is correct or not. If the existence of cluster formation is confirmed, a new property of nuclear matter will be revealed.

Acknowledgements

The authors appreciate the cooperation of Dr. T. Endo and Mr. Y. Narita received in the early stages of this study. This study was supported by a Waseda University Grant for Special Research Projects 2001A-620 and 2003A-628, a Grant-in-Aid for the 21st century COE program “Holistic Research and Education Center for Physics of Self-organizing Systems” at Waseda University, and a Grant-in-Aid from the Scientific Research Fund of the JSPS (No. 18540291). Most of the numerical calculations were performed with a SR8000/MPP at the Information Technology Center of the University of Tokyo.

Appendix A

— Spin-Polarized Neutron Matter with Fictitious Potentials —

In this appendix, we give the results of calculations for partially spin-polarized neutron matter with fictitious two-body nuclear potentials. It is not the purpose of this calculation to investigate the properties of real neutron matter. Rather, the purpose is to obtain information regarding the appearance of the new term studied in §4. Here, the two-body nuclear potential $V_s(r)$ ($s = 0, 1$) is taken to be of a purely central type. Then, the approximate energy expression given in Eq. (2·2) is appropriate, with the last term modified as explained in §2. We use the triplet-odd central component of the AV18 potential $V_{C11}(r)$ for both $s = 0$ and 1 with the modification explained below. The reason we do not use the singlet-even component of the AV18 potential as $V_0(r)$ is that, if it is used, the energy takes a large negative value. The modification of $V_{C11}(r)$ is as follows. The component $V_{C11}(r)$ is composed of three parts, as shown in Eq. (3·32), among which we multiply the intermediate and one-pion-exchange parts (V_p^I and V_p^π) by $C_1 = 0.9$ for the spin-triplet state and by $C_0 = 1, 1.1$ or 1.2 for the spin-singlet state. It should be noted that for $C_0 = 1.2$, the two-neutron system has a bound state, while for $C_0 = 1$ and 1.1 it has no bound state. The threshold for bound-state formation is $C_0 \approx 1.14$. We conjecture that the formation of a spin-singlet two-neutron bound state in spin-polarized neutron matter has some properties in common with the formation of self-mirror nuclei in asymmetric nuclear matter. Here, we point out that the numerical calculations for spin-polarized neutron matter are much simpler than those for spin-unpolarized asymmetric nuclear matter.

The results of the variational calculations for this spin-polarized fictitious neutron matter at $\rho = 0.16 \text{ fm}^{-3}$ are displayed in Fig. 15. There, the normalized energy

ε defined as

$$\varepsilon(\kappa) \equiv [E(\rho, \kappa)/N - E(\rho, \kappa = 0)/N] / [E(\rho, \kappa = 1)/N - E(\rho, \kappa = 0)/N] \quad (\text{A}\cdot 1)$$

is plotted as a function of κ^2 , where κ is the degree of polarization, defined by $\kappa = (\rho_u - \rho_d)/\rho$, with ρ_u and ρ_d being the number densities of spin-up and spin-down neutrons, respectively. In Fig. 15, we see the change in the characteristics of the curves for ε as C_0 varies. For $C_0 = 1$, the curve is almost straight, which means that the normalized energy is accurately approximated by a quadratic function of κ , or, if higher accuracy is required, by a power series in κ^2 . For $C_0 = 1.1$, deviation of the curve from a line becomes discernible, and for $C_0 = 1.2$, the deviation is more marked even in the very small neighborhood of $\kappa = 0$. This shows that, in order to represent this behavior, a term similar to the new term explained in §4 is necessary, and it also strongly suggests that this phenomenon is caused by cluster formation. Here, we comment on the observation that the curve for $C_0 = 1.1$ deviates, though slightly, from a line. The value $C_0 = 1.1$ is below the threshold of bound-state formation. Considering this point, can we attribute the deviation from a line to cluster formation? We think that we can. The formation of clusters in matter is not the same as the formation of bound states in free space. Cluster formation depends on the environment, and in neutron matter there are various environments with various probabilities. Therefore, the “threshold” of cluster formation in matter is not a point, but has a certain width. From this consideration, the slight deviation of the curve for $C_0 = 1.1$ from a line is consistent with cluster formation.

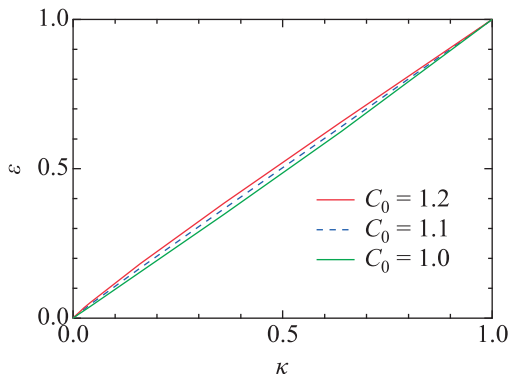


Fig. 15. Normalized energies $\varepsilon = [E/N(\rho, \kappa) - E/N(\rho, \kappa = 0)] / [E/N(\rho, \kappa = 1) - E/N(\rho, \kappa = 0)]$ for fictitious spin-polarized neutron matter.

We have one further comment, related to the modification of the energy expression made in §2. When we carried out the calculation for fictitious neutron matter with the old expression, Eq. (2-11), we encountered the difficulty that when we chose $C_1 = 1$ (not 0.9, as in the case considered in the above discussion) and $C_0 = 1$ at $\rho = 0.16 \text{ fm}^{-3}$, the calculated energy during the iteration decreased at $x \approx 0.8$ as if there were no lower bound, and the iteration did not converge. Thus, we were led to modify the energy expression, and after making this modification, our calculations were stable.

References

- 1) J. W. Clark, *Prog. Part. Nucl. Phys.* **2** (1979), 89.
- 2) W. Zuo, I. Bombaci and U. Lombardo, *Phys. Rev. C* **60** (1999), 024605.
D. Alonso and F. Sammarruca, *Phys. Rev. C* **67** (2003), 054301.
- 3) A. Akmal, V. R. Pandharipande and D. G. Ravenhall, *Phys. Rev. C* **58** (1998), 1804.
- 4) I. E. Lagaris and V. R. Pandharipande, *Nucl. Phys. A* **369** (1981), 470.
- 5) G. H. Bordbar and M. Modarres, *Phys. Rev. C* **57** (1998), 714.

- 6) M. Takano and M. Yamada, *Prog. Theor. Phys.* **91** (1994), 1149.
- 7) M. Takano and M. Yamada, *Prog. Theor. Phys.* **100** (1998), 745.
- 8) M. Takano, T. Endo, R. Kimura and M. Yamada, *Prog. Theor. Phys.* **109** (2003), 213.
- 9) M. Takano and M. Yamada, *Prog. Theor. Phys.* **88** (1992), 1131.
- 10) R. A. Aziz, V. P. S. Nain, J. S. Carley, W. L. Taylor and G. T. McConville, *J. Chem. Phys.* **70** (1979), 4330.
- 11) R. B. Wiringa, V. G. J. Stoks and R. Schiavilla, *Phys. Rev. C* **51** (1995), 38.
- 12) F. Iwamoto and M. Yamada, *Prog. Theor. Phys.* **17** (1957), 543.
- 13) M. Takano, *Prog. Theor. Phys.* **104** (2000), 185.
- 14) I. E. Lagaris and V. R. Pandharipande, *Nucl. Phys. A* **359** (1981), 349.
- 15) R. B. Wiringa, V. Fiks and A. Fabrocini, *Phys. Rev. C* **38** (1988), 1010.
- 16) M. Takano, *Prog. Theor. Phys. Suppl. No. 156* (2004), 141.
- 17) H. Koura, T. Tachibana, M. Uno and M. Yamada, *Prog. Theor. Phys.* **113** (2005), 305.